Research Paper https://doi.org/10.7733/jnfcwt.2021.19.2.187

Temperature and Concentration Dependencies of Chemical Equilibrium for Reductive Dissolution of Magnetite Using Oxalic Acid

Byung-Chul Lee[1,*] and Wonzin Oh[2]
[1]*Hannam University, 1646, Yuseong-daero, Yuseong-gu, Daejeon 34054, Republic of Korea*
[2]*Kyungpook National University, 80, Daehak-ro, Buk-gu, Daegu 41566, Republic of Korea*

(Received December 30, 2020 / Revised March 2, 2021 / Approved March 15, 2021)

Chemical equilibrium calculations for multicomponent aqueous systems involving the reductive dissolution of magnetite (Fe_3O_4) with oxalic acid ($H_2C_2O_4$) were performed using the HSC Chemistry® version 9. They were conducted with an aqueous solution model based on the Pitzer's approach of one molality aqueous solution. The change in the amounts and activity coefficients of species and ions involved in the reactions as well as the solution pH at equilibrium was calculated while changing the amounts of raw materials (Fe_3O_4 and $H_2C_2O_4$) and the system temperature from 25°C to 125°C. In particular, the conditions under which Fe_3O_4 is completely dissolved at high temperatures were determined by varying the raw amount of $H_2C_2O_4$ and the temperature for a given raw amount of Fe_3O_4 fed into the aqueous solution. When the raw amount of $H_2C_2O_4$ added was small for a given raw amount of Fe_3O_4, no undissolved Fe_3O_4 was present in the solution and the pH of the solution increased significantly. The formation of ferrous oxalate complex (FeC_2O_4) was observed. The equilibrium amount of FeC_2O_4 decreased as the raw amount of $H_2C_2O_4$ increased.

Keywords: Chemical decontamination, Chemical equilibrium, Reductive dissolution, Magnetite, Oxalic acid

*Corresponding Author.
Byung-Chul Lee, Hannam University, E-mail: bclee@hnu.kr, Tel: +82-42-629-8838

ORCID

Byung-Chul Lee	http://orcid.org/0000-0002-2935-8407	Wonzin Oh	http://orcid.org/0000-0002-3799-4200

1. Introduction

According to the nuclear power plant (NPP) decommissioning plan, the Kori Unit 1, one of the pressurized water reactors (PWR) in Korea, is expected to perform chemical decontamination of the reactor coolant system after permanent shutdown [1]. Decontamination of the reactor coolant system for decommissioning has been carried out at many overseas nuclear power plants [2-5], but none at all in Korea. Therefore, the development of the decontamination process technology for decommissioning the Kori Unit 1 is urgently needed [6]. In the case of nuclear power plants, as the number of years of operation increases, radioactive materials generated from the reactor are deposited in the form of a corrosion oxide layer on the surface of the coolant system, thereby increasing the level of radiation. Accordingly, it is necessary to reduce the radiation level by removing the corrosion oxide layer through decontamination before the decommissioning operation, since it causes heavy radiation exposure to workers during the decommission operation.

In general, the oxide layers deposited on the inner surface of structures of the coolant system of the PWR-type NPP are composed of metal oxides of iron, nickel, and chromium. Chemical decontamination by oxidative and reductive dissolutions has so far been recognized as the most effective method. The three key reactions for dissolving metal oxides consist of protonation to decompose oxygen bonds, reduction of Fe^{3+} ions to Fe^{2+} ions, and oxidation of Cr^{3+} ions to Cr^{6+} ions. Oxidative dissolution of chromium(III) oxide is carried out mainly with potassium permanganate or permanganic acid. Iron and nickel oxides are reduced and dissolved using aqueous solutions of acids like oxalic acid, citric acid, ethylelenediaminetetraacetic acid, and mixtures thereof. Thus, it is necessary to properly combine the oxidation and reduction processes when performing the decontamination of the coolant system [7]. Several permanganate processes using nitric permanganate (NP), alkaline permanganate (AP), and permanganic acid (HP) have been developed mainly for the oxidative dissolution. The reductive decontamination processes (CANDEREM, CITROX, LOMI, and CORD) have been developed to dissolve the iron oxides [8].

In this study, multi-component chemical equilibrium calculations were performed for heterogeneous aqueous systems that dissolve corrosion oxides using oxalic acid ($H_2C_2O_4$) as a reducing agent. Magnetite (Fe_3O_4) is considered as a target corrosion oxide in this work. By performing the equilibrium calculations using a Pitzer-based aqueous solution model that can be applied to aqueous electrolytes containing ions, the effect of the input amount of Fe_3O_4 and $H_2C_2O_4$ raw materials on the equilibrium amounts and activity coefficients of chemical species and ions involved in the dissolution reactions was investigated at various temperatures. The pH changes and the formation of ferrous/ferric oxalates were studied as well.

The scope of the work in this manuscript is to clarify the proposed dissolution systems in the thermodynamic perspective. From many experimental studies we have been aware of dissolution kinetics of the corrosion oxides in the reductive dissolution systems. The kinetic variation is actually not correlated with the thermodynamic consideration. Since the reductive dissolution reactions are greatly influenced by kinetics, it is revealed that the interpretation of the reactions through the equilibrium calculations has limitations.

2. Reaction Mechanism and Method of Calculations

The reductive dissolution using a reducing agent in the NPP chemical decontamination is to dissolve transition metal ions from the corrosion oxides deposited on the structure surfaces in the coolant system. In this work, only oxalic acid is used as a strong reducing agent which transfer electrons to Fe^{3+} ions to be reduced to Fe^{2+} ions. The reductive decontamination of magnetite with oxalic acid is a reaction mechanism in which three reaction steps occur simultaneously: (a) acidic dissolution of magnetite, (b) reduction of dissolved ferric ions by oxalic acid, and (c) complex formation of the dissolved ferrous ions with the oxalate. The reactions for the acidic dissolution of magnetite are as follows:

$$Fe_3O_4 + 2H^+ \rightarrow Fe^{2+} + Fe_2O_3 + H_2O \tag{1}$$

$$Fe_2O_3 + 6H^+ \rightarrow 2Fe^{3+} + 3H_2O \tag{2}$$

$$Fe_3O_4 + 8H^+ \rightarrow Fe^{2+} + 2Fe^{3+} + 4H_2O \tag{3}$$

Hydrogen ions (H^+) are provided by the dissociation of oxalic acid:

$$H_2C_2O_4 \rightarrow H^+ + HC_2O_4^- \tag{4}$$

$$H_2C_2O_4^- \rightarrow H^+ + C_2O_4^{2-} \tag{5}$$

Fe^{3+} ions are reduced to Fe^{2+} ions by electrons generated by the decomposition of oxalic acid:

$$H_2C_2O_4 \rightarrow 2H^+ + 2CO_2\ (g) + 2e^- \tag{6}$$

$$2Fe^{3+} + 2e^- \rightarrow 2Fe^{2+} \tag{7}$$

$$2Fe^{3+} + H_2C_2O_4 \rightarrow 2Fe^{2+} + 2CO_2\ (g) + 2H^+ \tag{8}$$

Combining the reactions (3) and (7) gives

$$Fe_3O_4 + 8H^+ + 2e^- \rightarrow 3Fe^{2+} + 4H_2O \tag{9}$$

From reactions (3) and (8), the acidic and reductive dissolution of magnetite by oxalic acid becomes:

$$Fe_3O_4 + H_2C_2O_4 + 6H^+ \rightarrow 3Fe^{2+} + 2CO_2\ (g) + 4H_2O \tag{10}$$

Plausible reaction schemes for the formation of complexes of ferric/ferrous ions with oxalate are as follows:

$$Fe^{2+} + H_2C_2O_4 \rightarrow FeC_2O_4 + 2H^+ \tag{11}$$

$$Fe^{3+} + H_2C_2O_4 \rightarrow FeC_2O_4^+ + 2H^+ \tag{12}$$

$$Fe^{3+} + H_2C_2O_4 \rightarrow FeHC_2O_4^{2+} + H^+ \tag{13}$$

Finally, from reactions (10) and (11), the dissolution reaction of magnetite by oxalic acid can be summarized as follows

$$Fe_3O_4 + 4H_2C_2O_4 \rightarrow 3FeC_2O_4 + 2CO_2\ (g) + 4H_2O \tag{14}$$

The calculations of multicomponent chemical equilibria in an aqueous system uses the Gibbs free energy minimization principle [9-11]. The theories and methods of the chemical equilibrium calculations are described in detail in the author's previous publication [12]. The expressions of the activity coefficients in electrolyte solutions and the model equations are given as well [13-16]. In this study, a semi-experimental model developed by Pitzer [9] and later modified by Harvie et al. [10] was used as a thermodynamic model suitable for calculating the activity coefficients of species and ions in a multicomponent aqueous solution. The calculations for the aqueous systems covered in this study are based on 1 molality (= 55.5082 mole of H_2O).

The chemical equilibrium for the aqueous system of the reductive dissolution of magnetite using oxalic acid was calculated by using the GEM module in the HSC Chemistry® version 9 [17]. The GIBBS solver and the AQUA module were used to calculate the amounts and activity coefficients of neutrals and ions in the dissolution reactions at equilibrium by varying the concentration of raw materials and the temperature. Additionally, the change of the pH values of the aqueous solution was observed.

Table 1. Conditions of equilibrium calculations for the reductive dissolution of magnetite by oxalic acid

Reagent	Phase	Raw amount [mol]
Fe_3O_4	solid	0.001, 0.005
$H_2C_2O_4$	aqueous	0.004~0.020
H_2O	aqueous	55.5082 (1 liter)
Temperature		25~125℃
Pressure		1 bar

Table 2. Chemical species and ions involved in the dissolution reactions of magnetite by oxalic acid

Phase	Species and ion
solid	Fe_3O_4, Fe_2O_3
aqueous	H_2O, $H_2C_2O_4$, H^+, OH^-, $HC_2O_4^-$, $C_2O_4^{2-}$, Fe^{3+}, Fe^{2+}, FeC_2O_4, $FeC_2O_4^+$, $FeHC_2O_4^{2+}$
gas	CO_2

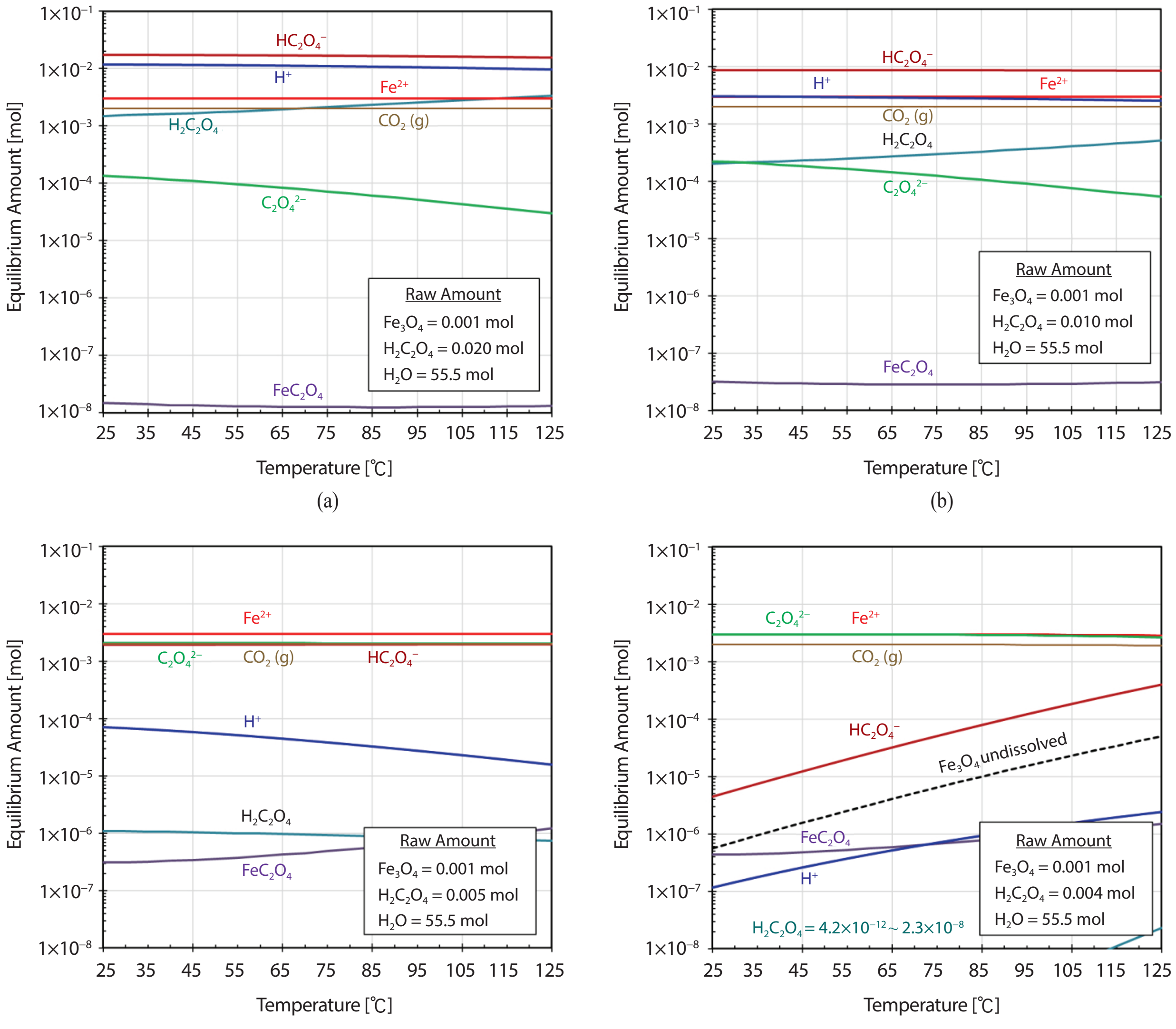

(a) (b)

(c) (d)

Fig. 1. Effect of raw amount of $H_2C_2O_4$ on equilibrium amounts of key species and ions as a function of temperature in the reductive dissolution of magnetite with oxalic acid. Raw amount of $H_2C_2O_4$ in mole is given inside each figure. Raw amount of Fe_3O_4 is kept constant at 0.001 mol. The equilibrium amounts of Fe^{3+} are not included in the figures since they are negligibly small.

Table 3. Results of equilibrium calculations for the Fe_3O_4-$H_2C_2O_4$-H_2O system: raw amount of Fe_3O_4 = 0.001 mol; raw amount of $H_2C_2O_4$ = 0.020 mol

Data Type	Species or ion	Phase	Unit	Temperature [°C]										
				25	35	45	55	65	75	85	95	105	115	125
Raw Amount	H_2O	aqueous	mol	55.5082	55.5082	55.5082	55.5082	55.5082	55.5082	55.5082	55.5082	55.5082	55.5082	55.5082
	$H_2C_2O_4$(l)	aqueous	mol	0.020	0.020	0.020	0.020	0.020	0.020	0.020	0.020	0.020	0.020	0.020
	Fe_3O_4(s)	solid	mol	0.001	0.001	0.001	0.001	0.001	0.001	0.001	0.001	0.001	0.001	0.001
Equilibrium Amount	CO_2(g)	gas	mol	0.002	0.002	0.002	0.002	0.002	0.002	0.002	0.002	0.002	0.002	0.002
	H_2O	aqueous	mol	55.5122	55.5122	55.5122	55.5122	55.5122	55.5122	55.5122	55.5122	55.5122	55.5122	55.5122
	$H_2C_2O_4$(l)	aqueous	mol	1.493×10^{-3}	1.570×10^{-3}	1.670×10^{-3}	1.793×10^{-3}	1.939×10^{-3}	2.110×10^{-3}	2.307×10^{-3}	2.530×10^{-3}	2.781×10^{-3}	3.061×10^{-3}	3.372×10^{-3}
	Fe^{3+}	aqueous	mol	1.039×10^{-21}	1.423×10^{-21}	1.888×10^{-21}	2.433×10^{-21}	3.057×10^{-21}	3.753×10^{-21}	4.510×10^{-21}	5.313×10^{-21}	6.146×10^{-21}	6.985×10^{-21}	7.807×10^{-21}
	Fe^{2+}	aqueous	mol	3.000×10^{-3}	3.000×10^{-3}	3.000×10^{-3}	3.000×10^{-3}	3.000×10^{-3}	3.000×10^{-3}	3.000×10^{-3}	3.000×10^{-3}	3.000×10^{-3}	3.000×10^{-3}	3.000×10^{-3}
	FeC_2O_4	aqueous	mol	1.483×10^{-8}	1.400×10^{-8}	1.341×10^{-8}	1.300×10^{-8}	1.271×10^{-8}	1.254×10^{-8}	1.247×10^{-8}	1.250×10^{-8}	1.262×10^{-8}	1.285×10^{-8}	1.319×10^{-8}
	FeC_2O_4+	aqueous	mol	4.435×10^{-20}	3.500×10^{-20}	2.809×10^{-20}	2.287×10^{-20}	1.886×10^{-20}	1.574×10^{-20}	1.328×10^{-20}	1.132×10^{-20}	9.744×10^{-21}	8.474×10^{-21}	7.444×10^{-21}
	$FeHC_2O_4^{2+}$	aqueous	mol	1.294×10^{-22}	2.328×10^{-22}	4.036×10^{-22}	6.760×10^{-22}	1.096×10^{-21}	1.726×10^{-21}	2.644×10^{-21}	3.948×10^{-21}	5.762×10^{-21}	8.230×10^{-21}	1.153×10^{-20}
	H^+	aqueous	mol	1.164×10^{-2}	1.155×10^{-2}	1.144×10^{-2}	1.130×10^{-2}	1.114×10^{-2}	1.096×10^{-2}	1.075×10^{-2}	1.052×10^{-2}	1.026×10^{-2}	9.975×10^{-3}	9.658×10^{-3}
	OH^-	aqueous	mol	1.191×10^{-12}	2.472×10^{-12}	4.797×10^{-12}	8.782×10^{-12}	1.526×10^{-11}	2.533×10^{-11}	4.034×10^{-11}	6.188×10^{-11}	9.178×10^{-11}	1.320×10^{-10}	1.847×10^{-10}
	$C_2O_4^{2-}$	aqueous	mol	1.336×10^{-4}	1.221×10^{-4}	1.093×10^{-4}	9.629×10^{-5}	8.367×10^{-5}	7.189×10^{-5}	6.120×10^{-5}	5.168×10^{-5}	4.333×10^{-5}	3.610×10^{-5}	2.991×10^{-5}
	$HC_2O_4^-$	aqueous	mol	1.737×10^{-2}	1.731×10^{-2}	1.722×10^{-2}	1.711×10^{-2}	1.698×10^{-2}	1.682×10^{-2}	1.663×10^{-2}	1.642×10^{-2}	1.618×10^{-2}	1.590×10^{-2}	1.560×10^{-2}
	Fe_3O_4(s)	solid	mol	0.0000	0.0000	0.0000	0.0000	0.0000	0.0000	0.0000	0.0000	0.0000	0.0000	0.0000
	Fe_2O_3(s)	solid	mol	0.0000	0.0000	0.0000	0.0000	0.0000	0.0000	0.0000	0.0000	0.0000	0.0000	0.0000
Activity coefficient	CO_2(g)	gas	-	1.0000	1.0000	1.0000	1.0000	1.0000	1.0000	1.0000	1.0000	1.0000	1.0000	1.0000
	H_2O	aqueous	-	1.0000	1.0000	1.0000	1.0000	1.0000	1.0000	1.0000	1.0000	1.0000	1.0000	1.0000
	$H_2C_2O_4$(l)	aqueous	-	1.0006	1.0006	1.0006	1.0006	1.0006	1.0006	1.0006	1.0006	1.0006	1.0006	1.0006
	Fe^{3+}	aqueous	-	0.2542	0.2487	0.2431	0.2373	0.2314	0.2253	0.2191	0.2128	0.2065	0.2001	0.1938
	Fe^{2+}	aqueous	-	0.5442	0.5390	0.5336	0.5279	0.5220	0.5158	0.5095	0.5029	0.4962	0.4893	0.4824
	FeC_2O_4	aqueous	-	1.0006	1.0006	1.0006	1.0006	1.0006	1.0006	1.0006	1.0006	1.0006	1.0006	1.0006
	$FeC_2O_4^+$	aqueous	-	0.8593	0.8572	0.8550	0.8528	0.8504	0.8478	0.8452	0.8425	0.8397	0.8367	0.8337
	$FeH_2O_4^{2+}$	aqueous	-	0.5442	0.5390	0.5336	0.5279	0.5220	0.5158	0.5095	0.5029	0.4962	0.4893	0.4824
	H^+	aqueous	-	0.8593	0.8572	0.8550	0.8528	0.8504	0.8478	0.8452	0.8425	0.8397	0.8367	0.8337
	OH^-	aqueous	-	0.8593	0.8572	0.8550	0.8528	0.8504	0.8478	0.8452	0.8425	0.8397	0.8367	0.8337
	$C_2O_4^{2-}$	aqueous	-	0.5442	0.5390	0.5336	0.5279	0.5220	0.5158	0.5095	0.5029	0.4962	0.4893	0.4824
	$HC_2O_4^-$	aqueous	-	0.8593	0.8572	0.8550	0.8528	0.8504	0.8478	0.8452	0.8425	0.8397	0.8367	0.8337
	Fe_3O_4(s)	solid	-	1.0000	1.0000	1.0000	1.0000	1.0000	1.0000	1.0000	1.0000	1.0000	1.0000	1.0000
	Fe_2O_3(s)	solid	-	1.0000	1.0000	1.0000	1.0000	1.0000	1.0000	1.0000	1.0000	1.0000	1.0000	1.0000
	pH of solution			2.000	2.004	2.009	2.016	2.023	2.032	2.041	2.052	2.064	2.078	2.094

3. Results and Discussion

Table 1 shows the conditions for calculating the chemical equilibrium for the reductive dissolution system of magnetite (Fe_3O_4) using oxalic acid ($H_2C_2O_4$). The concentration of oxalic acid concentration used for the NPP chemical decontamination is low and typically set to be 20 mM·L^{-1}. Equilibrium calculations were performed while varying the raw amounts of Fe_3O_4 and $H_2C_2O_4$ to observe the effect of the input amount of raw materials on the chemical equilibrium. The temperature dependence on the equilibrium was studied by performing the equilibrium calculations while changing the temperature of the system in the range of 25°C to 125°C at a given condition of the raw amounts. Note that the raw amount of H_2O is fixed at 55.5082 mole (1 liter) as our calculations are based on the aqueous solution of 1 molality. The pressure was kept constant at 1.0 bar for all calculations. Table 2 shows the chemical species and ions present in the solid, aqueous, and gas phases of the dissolution reactions of magnetite with oxalic acid.

Equilibrium calculations were repeatedly carried out at various input amounts of raw $H_2C_2O_4$ of 0.020 mol, 0.010 mol, 0.005 mol, and 0.004 mol. The results of calculations at two representative input amounts of raw $H_2C_2O_4$ (0.020 mol and 0.004 mol) are shown in Tables 3 and 4, respectively. Note that the input amount of raw Fe_3O_4 fed to the aqueous phase are set to be 0.001 mol for all the cases. The amounts and activity coefficients at equilibrium of species and ions participating in the reactions as well as the amounts of raw materials fed are shown at 10°C intervals in the temperature range from 25°C to 95°C. The pH values of aqueous solutions at equilibrium are also given as a function of temperature.

For four different amounts of $H_2C_2O_4$ fed to the aqueous phase, the changes in the equilibrium amounts of main chemical species and ions [CO_2(g), Fe^{2+}, Fe_3O_4(s) undissolved, $H_2C_2O_4$ unreacted, FeC_2O_4, $HC_2O_4^-$, $C_2O_4^{2-}$, H^+] are shown in Fig. 1 as a function of temperature. As shown in Fig. 1, when the input amount of the $H_2C_2O_4$ reducing agent was from 0.020 mol to 0.005 mol, the undissolved magnetite did not remain in the aqueous solution. In other words, when the concentration of the added $H_2C_2O_4$ reducing agent was 0.020~0.005 mol·L^{-1}, it can be seen that 0.001 mol of Fe_3O_4 was completely dissolved. Fe^{3+} ions were almost completely reduced to Fe^{2+} ions by oxalic acid. As can be seen in Table 4 and Fig. 1(d), the Fe_3O_4 undissolved was observed, when the input amount of raw $H_2C_2O_4$ was 0.004 mol. This indicates that 0.001 mol of Fe_3O_4 could not be completely dissolved when the concentration of the added $H_2C_2O_4$ reducing agent was 0.004 mol·L^{-1}. On the other hand, when the concentration of $H_2C_2O_4$ was 0.005 mol·L^{-1}, the Fe_3O_4 undissolved was not observed, which is shown in Fig. 1(c). Therefore, in order to completely reduce and dissolve 0.001 mol of Fe_3O_4, the concentration of the oxalic acid should be kept higher than 0.004 mol·L^{-1}.

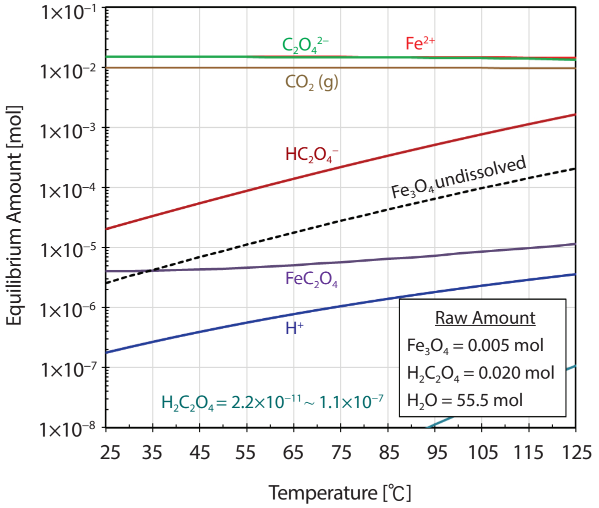

Fig. 2. Equilibrium amounts of key species and ions as a function of temperature in the reductive dissolution of magnetite with oxalic acid. Raw amounts of Fe_3O_4 and $H_2C_2O_4$ in mole are 0.005 and 0.020, respectively. The equilibrium amounts of Fe^{3+} are not included in the figures since they are negligibly small.

Table 4 and Fig. 2 show the results of the equilibrium calculations when the input amount of raw Fe_3O_4 was increased 5 times to 0.005 mol while the input amount of $H_2C_2O_4$ was maintained at 0.020 mol. Fe_3O_4 was not completely dissolved at all temperatures. Therefore, it is suggested that 0.020 mol of $H_2C_2O_4$ is insufficient to completely dissolve 0.005 mol of Fe_3O_4.

Table 4. Results of equilibrium calculations for the Fe_3O_4-$H_2C_2O_4$-H_2O system: raw amount of Fe_3O_4 = 0.001 mol; raw amount of $H_2C_2O_4$ = 0.004 mol

Data Type	Species or ion	Phase	Unit	Temperature [°C]										
				25	35	45	55	65	75	85	95	105	115	125
Raw Amount	H_2O	aqueous	mol	55.5082	55.5082	55.5082	55.5082	55.5082	55.5082	55.5082	55.5082	55.5082	55.5082	55.5082
	$H_2C_2O_4(l)$	aqueous	mol	0.004	0.004	0.004	0.004	0.004	0.004	0.004	0.004	0.004	0.004	0.004
	$Fe_3O_4(s)$	solid	mol	0.001	0.001	0.001	0.001	0.001	0.001	0.001	0.001	0.001	0.001	0.001
Equilibrium Amount	$CO_2(g)$	gas	mol	1.999×10^{-3}	1.998×10^{-3}	1.997×10^{-3}	1.995×10^{-3}	1.992×10^{-3}	1.987×10^{-3}	1.980×10^{-3}	1.969×10^{-3}	1.954×10^{-3}	1.931×10^{-3}	1.899×10^{-3}
	H_2O	aqueous	mol	55.5122	55.5122	55.5122	55.5122	55.5122	55.5122	55.5122	55.5121	55.5121	55.5121	55.5120
	$H_2C_2O_4(l)$	aqueous	mol	4.197×10^{-12}	1.130×10^{-11}	2.951×10^{-11}	7.483×10^{-11}	1.843×10^{-10}	4.414×10^{-10}	1.029×10^{-9}	2.334×10^{-9}	5.161×10^{-9}	1.111×10^{-8}	2.329×10^{-8}
	Fe^{3+}	aqueous	mol	1.731×10^{-22}	2.262×10^{-22}	2.834×10^{-22}	3.423×10^{-22}	4.003×10^{-22}	4.549×10^{-22}	5.036×10^{-22}	5.444×10^{-22}	5.753×10^{-22}	5.951×10^{-22}	6.030×10^{-22}
	Fe^{2+}	aqueous	mol	2.998×10^{-3}	2.997×10^{-3}	2.995×10^{-3}	2.992×10^{-3}	2.987×10^{-3}	2.980×10^{-3}	2.969×10^{-3}	2.953×10^{-3}	2.929×10^{-3}	2.895×10^{-3}	2.848×10^{-3}
	FeC_2O_4	aqueous	mol	4.352×10^{-7}	4.503×10^{-7}	4.817×10^{-7}	5.293×10^{-7}	5.939×10^{-7}	6.778×10^{-7}	7.841×10^{-7}	9.164×10^{-7}	1.079×10^{-6}	1.274×10^{-6}	1.504×10^{-6}
	$FeC_2O_4^+$	aqueous	mol	2.485×10^{-19}	2.052×10^{-19}	1.741×10^{-19}	1.509×10^{-19}	1.332×10^{-19}	1.194×10^{-19}	1.085×10^{-19}	9.964×10^{-20}	9.229×10^{-20}	8.602×10^{-20}	8.045×10^{-20}
	$FeHC_2O_4^{2+}$	aqueous	mol	6.853×10^{-27}	1.972×10^{-26}	5.356×10^{-26}	1.377×10^{-25}	3.366×10^{-25}	7.842×10^{-25}	1.747×10^{-24}	3.733×10^{-24}	7.664×10^{-24}	1.513×10^{-23}	2.876×10^{-23}
	H^+	aqueous	mol	1.178×10^{-7}	1.787×10^{-7}	2.624×10^{-7}	3.741×10^{-7}	5.194×10^{-7}	7.040×10^{-7}	9.335×10^{-7}	1.214×10^{-6}	1.549×10^{-6}	1.946×10^{-6}	2.406×10^{-6}
	OH^-	aqueous	mol	1.101×10^{-7}	1.493×10^{-7}	1.954×10^{-7}	2.477×10^{-7}	3.056×10^{-7}	3.679×10^{-7}	4.332×10^{-7}	4.997×10^{-7}	5.656×10^{-7}	6.288×10^{-7}	6.872×10^{-7}
	$C_2O_4^{2-}$	aqueous	mol	2.996×10^{-3}	2.993×10^{-3}	2.989×10^{-3}	2.982×10^{-3}	2.971×10^{-3}	2.955×10^{-3}	2.930×10^{-3}	2.892×10^{-3}	2.837×10^{-3}	2.758×10^{-3}	2.648×10^{-3}
	$HC_2O_4^-$	aqueous	mol	4.511×10^{-6}	7.520×10^{-6}	1.239×10^{-5}	2.014×10^{-5}	3.230×10^{-5}	5.107×10^{-5}	7.961×10^{-5}	1.223×10^{-4}	1.849×10^{-4}	2.748×10^{-4}	4.007×10^{-4}
	$Fe_3O_4(s)$	solid	mol	5.648×10^{-7}	9.437×10^{-7}	1.557×10^{-6}	2.533×10^{-6}	4.064×10^{-6}	6.426×10^{-6}	1.001×10^{-5}	1.537×10^{-5}	2.324×10^{-5}	3.452×10^{-5}	5.031×10^{-5}
	$Fe_2O_3(s)$	solid	mol	0.0000	0.0000	0.0000	0.0000	0.0000	0.0000	0.0000	0.0000	0.0000	0.0000	0.0000
Activity coefficient	$CO_2(g)$	gas	-	1.0000	1.0000	1.0000	1.0000	1.0000	1.0000	1.0000	1.0000	1.0000	1.0000	1.0000
	H_2O	aqueous	-	1.0000	1.0000	1.0000	1.0000	1.0000	1.0000	1.0000	1.0000	1.0000	1.0000	1.0000
	$H_2C_2O_4(l)$	aqueous	-	1.0001	1.0001	1.0001	1.0001	1.0001	1.0001	1.0001	1.0001	1.0001	1.0001	1.0001
	Fe^{3+}	aqueous	-	0.3443	0.3378	0.3310	0.3238	0.3164	0.3088	0.3011	0.2935	0.2861	0.2791	0.2730
	Fe^{2+}	aqueous	-	0.6226	0.6174	0.6118	0.6059	0.5997	0.5932	0.5866	0.5799	0.5734	0.5672	0.5616
	FeC_2O_4	aqueous	-	1.0001	1.0001	1.0001	1.0001	1.0001	1.0001	1.0001	1.0001	1.0001	1.0001	1.0001
	$FeC_2O_4^+$	aqueous	-	0.8884	0.8865	0.8845	0.8823	0.8801	0.8777	0.8752	0.8727	0.8703	0.8679	0.8658
	$FeH_2O_4^{2+}$	aqueous	-	0.6226	0.6174	0.6118	0.6059	0.5997	0.5932	0.5866	0.5799	0.5734	0.5672	0.5616
	H^+	aqueous	-	0.8884	0.8865	0.8845	0.8823	0.8801	0.8777	0.8752	0.8727	0.8703	0.8679	0.8658
	OH^-	aqueous	-	0.8884	0.8865	0.8845	0.8823	0.8801	0.8777	0.8752	0.8727	0.8703	0.8679	0.8658
	$C_2O_4^{2-}$	aqueous	-	0.6226	0.6174	0.6118	0.6059	0.5997	0.5932	0.5866	0.5799	0.5734	0.5672	0.5616
	$HC_2O_4^-$	aqueous	-	0.8884	0.8865	0.8845	0.8823	0.8801	0.8777	0.8752	0.8727	0.8703	0.8679	0.8658
	$Fe_3O_4(s)$	solid	-	1.0000	1.0000	1.0000	1.0000	1.0000	1.0000	1.0000	1.0000	1.0000	1.0000	1.0000
	$Fe_2O_3(s)$	solid	-	1.0000	1.0000	1.0000	1.0000	1.0000	1.0000	1.0000	1.0000	1.0000	1.0000	1.0000
	pH of solution			2.000	2.004	2.009	6.980	6.800	6.634	6.481	6.340	6.209	6.087	5.975

Table 5. Results of equilibrium calculations for the Fe_3O_4-$H_2C_2O_4$-H_2O system: raw amount of Fe_3O_4 = 0.005 mol; raw amount of $H_2C_2O_4$ = 0.020 mol

Data Type	Species or ion	Phase	Unit	Temperature [°C]										
				25	35	45	55	65	75	85	95	105	115	125
Raw Amount	H_2O	aqueous	mol	55.5082	55.5082	55.5082	55.5082	55.5082	55.5082	55.5082	55.5082	55.5082	55.5082	55.5082
	$H_2C_2O_4(l)$	aqueous	mol	0.020	0.020	0.020	0.020	0.020	0.020	0.020	0.020	0.020	0.020	0.020
	$Fe_3O_4(s)$	solid	mol	0.005	0.005	0.005	0.005	0.005	0.005	0.005	0.005	0.005	0.005	0.005
Equilibrium Amount	$CO_2(g)$	gas	mol	9.995×10^{-3}	9.991×10^{-3}	9.986×10^{-3}	9.978×10^{-3}	9.964×10^{-3}	9.944×10^{-3}	9.914×10^{-3}	9.870×10^{-3}	9.805×10^{-3}	9.713×10^{-3}	9.583×10^{-3}
	H_2O	aqueous	mol	55.5282	55.5282	55.5282	55.5282	55.5281	55.5281	55.5280	55.5279	55.5278	55.5276	55.5274
	$H_2C_2O_4(l)$	aqueous	mol	2.232×10^{-11}	5.930×10^{-11}	1.527×10^{-10}	3.815×10^{-10}	9.249×10^{-10}	2.178×10^{-9}	4.991×10^{-9}	1.114×10^{-8}	2.423×10^{-8}	5.142×10^{-8}	1.065×10^{-7}
	Fe^{3+}	aqueous	mol	9.203×10^{-22}	1.222×10^{-21}	1.556×10^{-21}	1.914×10^{-21}	2.281×10^{-21}	2.645×10^{-21}	2.992×10^{-21}	3.307×10^{-21}	3.575×10^{-21}	3.784×10^{-21}	3.920×10^{-21}
	Fe^{2+}	aqueous	mol	1.499×10^{-2}	1.498×10^{-2}	1.497×10^{-2}	1.496×10^{-2}	1.494×10^{-2}	1.491×10^{-2}	1.487×10^{-2}	1.480×10^{-2}	1.470×10^{-2}	1.456×10^{-2}	1.436×10^{-2}
	FeC_2O_4	aqueous	mol	4.042×10^{-6}	4.109×10^{-6}	4.314×10^{-6}	4.645×10^{-6}	5.103×10^{-6}	5.697×10^{-6}	6.442×10^{-6}	7.362×10^{-6}	8.480×10^{-6}	9.824×10^{-6}	1.142×10^{-5}
	$FeC_2O_4^{+}$	aqueous	mol	1.496×10^{-18}	1.222×10^{-18}	1.024×10^{-18}	8.769×10^{-19}	7.641×10^{-19}	6.757×10^{-19}	6.052×10^{-19}	5.481×10^{-19}	5.009×10^{-19}	4.613×10^{-19}	4.274×10^{-19}
	$FeHC_2O_4^{2+}$	aqueous	mol	7.900×10^{-26}	2.259×10^{-25}	6.092×10^{-25}	1.555×10^{-24}	3.771×10^{-24}	8.715×10^{-24}	1.927×10^{-23}	4.086×10^{-23}	8.331×10^{-23}	1.637×10^{-22}	3.102×10^{-22}
	H^{+}	aqueous	mol	1.761×10^{-7}	2.672×10^{-7}	3.924×10^{-7}	5.595×10^{-7}	7.767×10^{-7}	1.053×10^{-6}	1.396×10^{-6}	1.815×10^{-6}	2.318×10^{-6}	2.911×10^{-6}	3.600×10^{-6}
	OH^{-}	aqueous	mol	9.434×10^{-8}	1.285×10^{-7}	1.689×10^{-7}	2.153×10^{-7}	2.671×10^{-7}	3.234×10^{-7}	3.831×10^{-7}	4.447×10^{-7}	5.066×10^{-7}	5.669×10^{-7}	6.236×10^{-7}
	$C_2O_4^{2-}$	aqueous	mol	1.498×10^{-2}	1.497×10^{-2}	1.495×10^{-2}	1.492×10^{-2}	1.487×10^{-2}	1.480×10^{-2}	1.469×10^{-2}	1.454×10^{-2}	1.431×10^{-2}	1.399×10^{-2}	1.353×10^{-2}
	$HC_2O_4^{-}$	aqueous	mol	2.056×10^{-5}	3.397×10^{-5}	5.543×10^{-5}	8.923×10^{-5}	1.416×10^{-4}	2.215×10^{-4}	3.416×10^{-4}	5.191×10^{-4}	7.774×10^{-4}	1.146×10^{-3}	1.663×10^{-3}
	$Fe_3O_4(s)$	solid	mol	2.580×10^{-6}	4.264×10^{-6}	6.957×10^{-6}	1.120×10^{-5}	1.776×10^{-5}	2.778×10^{-5}	4.283×10^{-5}	6.507×10^{-5}	9.741×10^{-5}	1.436×10^{-4}	2.083×10^{-4}
	$Fe_2O_3(s)$	solid	mol	0.0000	0.0000	0.0000	0.0000	0.0000	0.0000	0.0000	0.0000	0.0000	0.0000	0.0000
Activity coefficient	$CO_2(g)$	gas	-	1.0000	1.0000	1.0000	1.0000	1.0000	1.0000	1.0000	1.0000	1.0000	1.0000	1.0000
	H_2O	aqueous	-	1.0002	1.0002	1.0002	1.0002	1.0002	1.0002	1.0002	1.0002	1.0002	1.0002	1.0002
	$H_2C_2O_4(l)$	aqueous	-	1.0005	1.0005	1.0005	1.0005	1.0005	1.0005	1.0005	1.0005	1.0005	1.0005	1.0005
	Fe^{3+}	aqueous	-	0.1131	0.1088	0.1043	0.0997	0.0951	0.0904	0.0857	0.0812	0.0768	0.0728	0.0691
	Fe^{2+}	aqueous	-	0.3797	0.3732	0.3663	0.3591	0.3515	0.3437	0.3357	0.3277	0.3198	0.3121	0.3050
	FeC_2O_4	aqueous	-	1.0005	1.0005	1.0005	1.0005	1.0005	1.0005	1.0005	1.0005	1.0005	1.0005	1.0005
	$FeC_2O_4^{+}$	aqueous	-	0.7853	0.7819	0.7783	0.7744	0.7703	0.7660	0.7615	0.7569	0.7523	0.7477	0.7434
	$FeH_2O_4^{2+}$	aqueous	-	0.3797	0.3732	0.3663	0.3591	0.3515	0.3437	0.3357	0.3277	0.3198	0.3121	0.3050
	H^{+}	aqueous	-	0.7853	0.7819	0.7783	0.7744	0.7703	0.7660	0.7615	0.7569	0.7523	0.7477	0.7434
	OH^{-}	aqueous	-	0.7853	0.7819	0.7783	0.7744	0.7703	0.7660	0.7615	0.7569	0.7523	0.7477	0.7434
	$C_2O_4^{2-}$	aqueous	-	0.3797	0.3732	0.3663	0.3591	0.3515	0.3437	0.3357	0.3277	0.3198	0.3121	0.3050
	$HC_2O_4^{-}$	aqueous	-	0.7853	0.7819	0.7783	0.7744	0.7703	0.7660	0.7615	0.7569	0.7523	0.7477	0.7434
	$Fe_3O_4(s)$	solid	-	1.0000	1.0000	1.0000	1.0000	1.0000	1.0000	1.0000	1.0000	1.0000	1.0000	1.0000
	$Fe_2O_3(s)$	solid	-	1.0000	1.0000	1.0000	1.0000	1.0000	1.0000	1.0000	1.0000	1.0000	1.0000	1.0000
	pH of solution			6.859	6.680	6.515	6.363	6.223	6.093	5.973	5.862	5.758	5.662	5.572

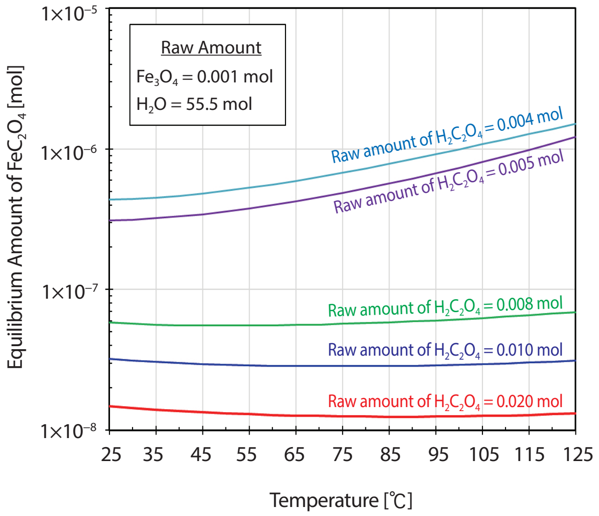

Fig. 3. Results of equilibrium calculations for the Fe_3O_4-$H_2C_2O_4$-H_2O system: the effect of the raw amount of $H_2C_2O_4$ on the amount of FeC_2O_4 formation in equilibrium as a function of temperature.

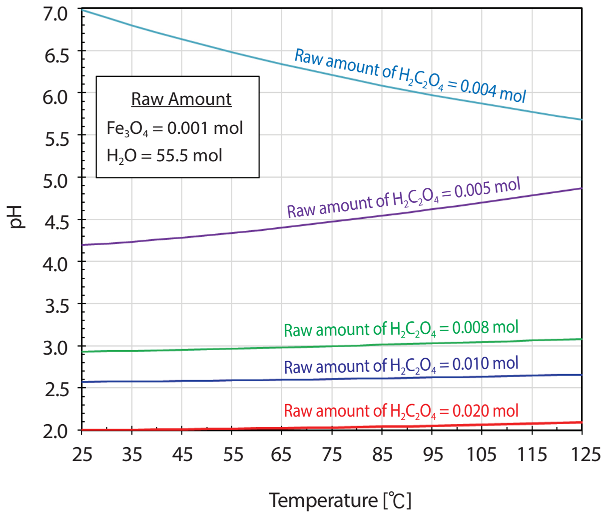

Fig. 4. Results of equilibrium calculations for the Fe_3O_4-$H_2C_2O_4$-H_2O system: the effect of the raw amount of $H_2C_2O_4$ on the pH of the aqueous solution in equilibrium as a function of temperature.

The equilibrium amounts of ferrous/ferric oxalates (FeC_2O_4, $FeC_2O_4^+$, $FeHC_2O_4^{2+}$), which can be generated by the complex formation of ferrous/ferric ions and $HC_2O_4^-$ or $C_2O_4^{2-}$ ions, was calculated. In particular, the results for the equilibrium amount of FeC_2O_4 are schematically shown in Fig. 3. It can be seen that a very small amount (10^{-8}~10^{-5} mol of order of magnitude) of FeC_2O_4 was produced, and the amount of FeC_2O_4 produced decreased as the input amount of $H_2C_2O_4$ added increased. As can be seen in Tables 3 to 5, $FeC_2O_4^+$ and $FeHC_2O_4^{2+}$ were hardly produced.

Fig. 4 shows the change in the pH of aqueous solution as a function of temperature for the Fe_3O_4-$H_2C_2O_4$-H_2O system at various amounts of raw $H_2C_2O_4$ added into the aqueous solution. Not surprisingly, when compared at the same temperature, the pH of the solution increased markedly as the raw amount of $H_2C_2O_4$ decreased. In addition, in the case of the raw amount of $H_2C_2O_4$ in the range of 0.020 to 0.005 mol, the pH of the solution gradually increased as the temperature increased. However, when the raw amount of $H_2C_2O_4$ was 0.004 mol, the pH of the solution decreased as the temperature increased, which seems to be due to the fact that Fe_3O_4 was not completely dissolved.

4. Conclusions

The chemical equilibrium of the aqueous system for the reductive dissolution of magnetite with oxalic acid (Fe_3O_4-$H_2C_2O_4$-H_2O) was calculated at high temperatures up to 125°C, by using the HSC Chemistry® version 9 software. This study focused on the effect of the amounts of raw materials fed into the aqueous phase on the equilibrium amounts of species and ions involved in the reductive dissolution reactions and the pH of the aqueous solution. In particular, we observed the conditions in which Fe_3O_4 was completely dissolved as well as the equilibrium amount of FeC_2O_4 complex produced.

For the raw amount of Fe_3O_4 of 0.001 mol, when the raw amount of $H_2C_2O_4$ was from 0.020 mol to 0.005 mol, no Fe_3O_4 undissolved was present in the solution and Fe^{3+} ions were almost completely reduced to Fe^{2+} ions by $H_2C_2O_4$. On the other hand, at the raw amount of $H_2C_2O_4$ as low as 0.004 mol, Fe_3O_4 was not completely dissolved. The pH of the solution increased with increasing the solution temperature. The equilibrium amount of FeC_2O_4 produced decreased as the raw amount of $H_2C_2O_4$ increased. The calculation results obtained from this work provide information for the input amounts of the raw materials and the pH values of the aqueous solution in which Fe_3O_4 is completely dissolved at high temperatures.

Acknowledgements

This work was supported by the Korea Institute of Energy Technology Evaluation and Planning (KETEP) and the Ministry of Trade, Industry and Energy (MOTIE) of the Republic of Korea (No. 20191510301310).

REFERENCES

[1] C. Kim and H. Kim, “Study on Chemical Decontamination Process Based on Permanganic Acid-Oxalic Acid to Remove Oxide Layer Deposited in Primary System of Nuclear Power Plant”, J. Nucl. Fuel Cycle Waste Technol., 17(1), 15-28 (2019).

[2] H. Ocken. Decontamination Handbook, Economic Policy Research Institute Report, TR-112352 (1999).

[3] R. McGrath and J. Cabrera. Nuclear Power Plant Full System Chemical Decontamination Experience Report, Economic Policy Research Institute Report, 21-43, TR-1019230 (2009).

[4] T.A. Beaman and J.L. Smee. Evaluation of the Decontamination of the Reactor Coolant Systems at Maine Yankee and Connecticut Yankee, Economic Policy Research Institute Report, TR-112092 (1999).

[5] D. Well. Recent Chemical Decontamination Experience, Economic Policy Research Institute Report, 3002000555 (2013).

[6] D.H. Lee. Analysis of Basic Requirements for Kori-1 Full System Decontamination, Korea Hydro & Nuclear Power Central Research Institute Report, 2015-50003339-0488TC (2015).

[7] J.Y. Jung, S.Y. Park, H.J. Won, S.B. Kim, W.K. Choi, J.K. Moon, and S.J. Park, “Corrosion Properties of Inconel-600 and 304 Stainless Steel in New Oxidative and Reductive Decontamination Reagent”, Met. Mater. Int., 21(4), 678-685 (2015).

[8] J.K. Moon, S.B. Kim, W.K. Choi, B.S. Choi, D.Y. Chung, and B.K. Seo, “The Status and Prospect of Decommissioning Technology Development at KAERI”, J. Nucl. Fuel Cycle Waste Technol., 17(2), 139-165 (2019).

[9] K.S. Pitzer, “Thermodynamics of Electrolytes. I. Theoretical Basis and General Equations”, J. Phys. Chem., 77, 268-277 (1973).

[10] C.E. Harvie and J.H. Weare, “The Prediction of Mineral Solubilities in Natural Waters: the Na-K-Mg-Ca-Cl-SO4-H_2O System From Zero to High Concentration at 25°C”, Geochim. Cosmochim. Acta, 44(7), 981-997 (1980).

[11] C.E. Harvie, N. Møller, and J.H. Weare, “The Prediction of Mineral Solubilities in Natural Waters: The Na-K-Mg-Ca-H-Cl-SO_4-OH-HCO_3-CO_3-CO_2-H_2O System to High Ionic Strengths at 25°C”, Geochim. Cosmochim. Acta, 48(4), 723-751 (1984).

[12] B.C. Lee, S.B. Kim, and J.K. Moon, “Equilibrium Calculations for HyBRID Decontamination of Magnetite: Effect of Raw Amount of $CuSO_4$ on Cu_2O Formation”, Nucl. Eng. Technol., 52(11), 2543-2551 (2020).

[13] K.S. Pitzer, Thermodynamics, 3rd ed., McGraw-Hill, New York (1995).

[14] K.S. Pitzer, Activity Coefficients in Electrolyte Solutions, 2nd ed., CRC Press, Boca Raton, FL (1979).

[15] J.M. Prausnitz, R.N. Lichtenthaler, and E. Gomes de Azevedo, Molecular Thermodynamics of Fluid- Phase Equilibria, 3rd ed., Pearson Education, London (1999).

[16] J.F. Zemaitis, Jr., D.M. Clark, M. Rafal, and N.C. Scrivner, Handbook of Aqueous Electrolyte Thermodynamics, Wiley-AIChE, Hoboken, NJ (1986).

[17] HSC Chemistry Software, www.outotec.com.